E-field-induced polarization rotation in Pb (Mg 1/3 Nb 2/3) 1−x Ti x O 3 crystal

Chi-Shun Tu, I.-C. Shih, V. Hugo Schmidt, and R. Chien

Citation: Applied Physics Letters **83**, 1833 (2003); doi: 10.1063/1.1602558
View online: http://dx.doi.org/10.1063/1.1602558
View Table of Contents: http://scitation.aip.org/content/aip/journal/apl/83/9?ver=pdfcov
Published by the AIP Publishing

E-field-induced polarization rotation in $Pb(Mg_{1/3}Nb_{2/3})_{1-x}Ti_xO_3$ crystal

Chi-Shun Tu[a] and I.-C. Shih
Department of Physics, Fu Jen University, Taipei, Taiwan 242, Republic of China

V. Hugo Schmidt and R. Chien
Department of Physics, Montana State University, Bozeman, Montana 59717

(Received 21 April 2003; accepted 17 June 2003)

A sequence of field-induced phase transformations was observed by means of a polarizing microscope on a (111)-cut single crystal $Pb(Mg_{1/3}Nb_{2/3})_{0.67}Ti_{0.33}O_3$ at room temperature with an electric field applied along the [111] direction. As electric field increases, polarizations of the rhombohedral R domains whose polar directions are not along [111] rotate first toward a tetragonal T phase associated with 90° domain walls. Then the crystal gradually reaches total optical extinction for all polarizer angles at 12 kV/cm, indicating a single [111] rhombohedral R_{111} domain with polarization aligned with the electric field. These field-induced phase transformations are irreversible and proceed most likely through M_A-type monoclinic distortions, i.e., $R \rightarrow M_A \rightarrow T \rightarrow M_A \rightarrow R_{111}$. © *2003 American Institute of Physics.* [DOI: 10.1063/1.1602558]

Monoclinic (M) and orthorhombic (O) phases have been recently reported in both $Pb(Mg_{1/3}Nb_{2/3})_{1-x}Ti_xO_3$ (PMNTx) and $Pb(Zn_{1/3}Nb_{2/3})_{1-x}Ti_xO_3$ (PZNTx) systems, which depend strongly on Ti concentration, temperature range, strength of external electric (E) field, and crystallographic orientation.[1–10] Durbin *et al.* proposed, by x-ray diffraction, that under E field along ⟨001⟩ PZNT8% can no longer be rhombohedral (R), but that instead it is almost certainly monoclinic.[1] From the E-field dependent polarization, a metastable O phase was proposed in PZNT8% crystals oriented along ⟨001⟩, ⟨110⟩ and ⟨111⟩.[2] By synchrotron x-ray diffraction with E field applied along [001], various polarization paths of $R-M_C-T$ and $R-M_A-T$ were proposed in PZNT8% and PZNT4.5% crystals, respectively.[3] An O phase was observed in the PZNTx system for $x=8\%$ and $x=9\%$ after a prior E-field application along ⟨001⟩.[4]

With a prior poling along a (011)-cut PMNT33% crystal, an extra O phase between R and T phases was claimed from the dielectric result.[5] From polarization result, an E-field-induced transformation from ⟨111⟩ R to ⟨110⟩ O phase through M_B distortion was proposed on a (110)-cut PMNT30% crystal.[6] Based on synchrotron results, an M_A phase was observed in a (001)-cut PMNT35% crystal previously poled under an E field of 43 kV/cm.[7] However, unpoled and weakly poled PMNT35% samples exhibit an average R symmetry.[7] An M_C phase has so far been reported in PMNT only for powder and ceramic samples.[8–10] It is important to note that the effect of M_A-type polarization rotation will be largely canceled in randomly oriented ceramics.[11]

These phenomena give us a new insight into domain engineering for high piezoelectric performance in the PMNT system. However, the effect of an E field on polarization rotations is still not clear. One may ask how monoclinic distortions play a role in phase transformations under an E field. In this letter, E-field-dependent domain structures were investigated on a (111)-cut PMNT33% crystal.

The PMNT33% crystal was grown using a modified Bridgman method. The sample was cut perpendicular to the ⟨111⟩ direction. The domain structures were observed by using a Nikon E600POL polarizing microscope with a 0°/90° crossed polarizer/analyzer (P/A) pair. Transparent conductive films of indium tin oxide (ITO) were deposited on sample surfaces and the sample thickness is about 50 μm. The experimental configuration is illustrated in Ref. 12. A dc external E field was applied to the sample along [111]. All pictures in Figs. 1(a)–1(h) were observed under the crossed P/A pair. For comparison, the hysteresis loop is given in Fig. 1(i).

The propagation direction **k** of the polychromatic ''white'' light is along [111] for this work. The most information is obtained from observation of optical extinction, which occurs if all the following conditions are satisfied: (1) there must be no optical activity for the direction **k**, (2) either if **k** must lie along an optical axis, or if **k** is not along an optical axis, the incident **E** must lie along one of the two perpendicular axes in the plane perpendicular to **k** for which the optical-frequency permittivity is maximum or minimum. An analysis for the general extinction appears in Refs. 13 and 14.

The T and R phases have uniaxial strain tensors with principal axes and polarization **P** along ⟨001⟩ and ⟨111⟩, respectively. For the O phase observed in perovskites, the strain tensor is biaxial, with principal axes (for one example) along [101], $[10\bar{1}]$, and [010] and **P** along $\pm[101]$ or $\pm[10\bar{1}]$. Monoclinic cell strain tensors are biaxial, with one principal axis along ⟨001⟩ or ⟨110⟩, and the other two axes and **P** in arbitrary directions perpendicular to that axis. The ⟨001⟩ case corresponds to the cell based on the primitive unit cell ($Z=1$) for the cubic phase, while the ⟨110⟩ case corresponds to the cell based on the double-size O cell ($Z=2$).

Figure 2 shows the relations among the various phases and polarizations for the primitive unit cell and double-size O cell. A rectangle indicates the directions of tetragonal polarization vectors **P**. A triangle indicates directions for rhom-

[a]Author to whom correspondence should be addressed; electronic mail: phys1008@mails.fju.edu.tw

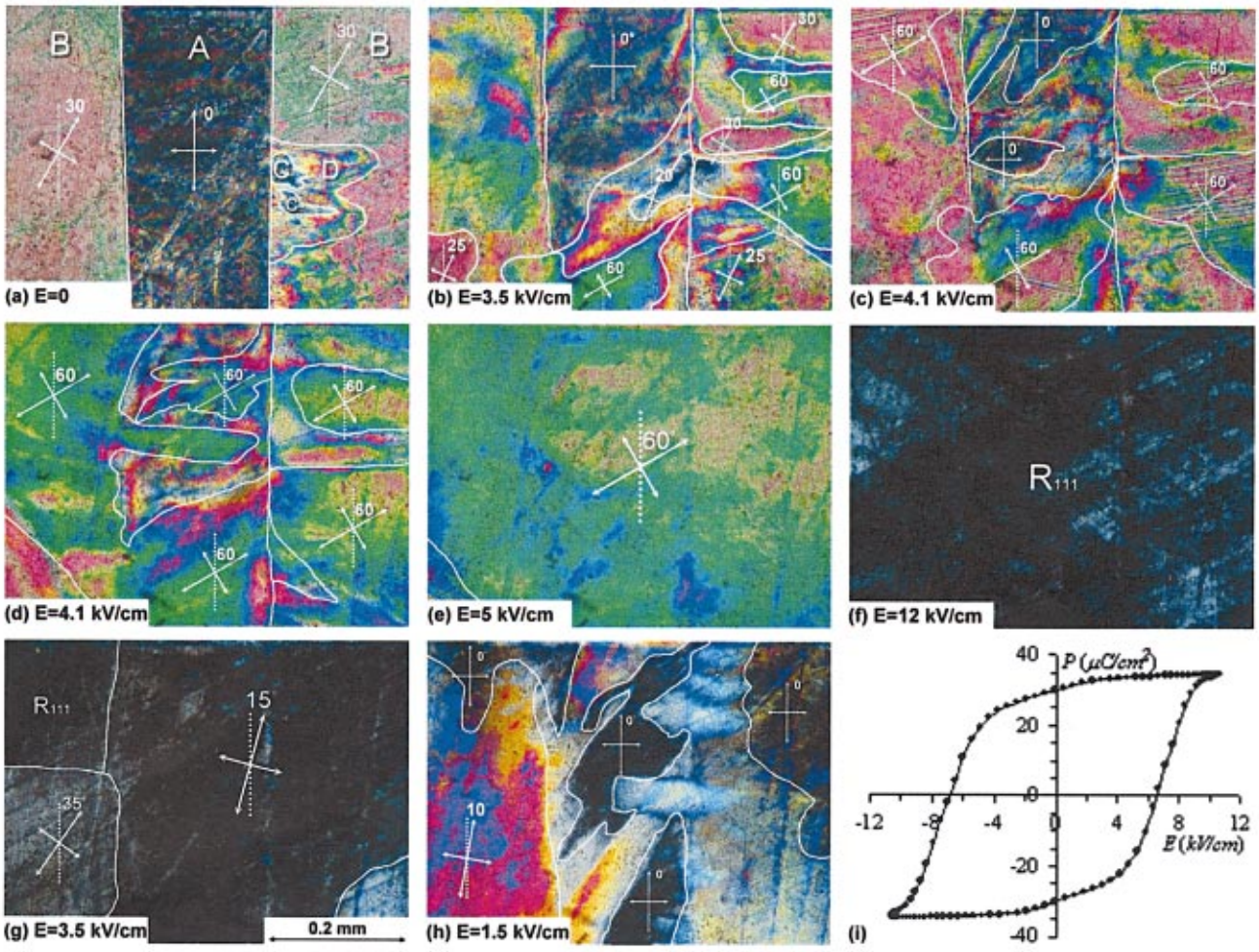

FIG. 1. (Color) (a)–(h) E-field dependent domain structures, (i) hysteresis loop of polarization vs E field obtained at room temperature.

bohedral **P**'s. A circle indicates directions for orthorhombic **P**'s. Solid, dash-dot and dashed lines run along all edges and face diagonals, indicating directions that polarizations can take for monoclinic cells based on the double-size orthorhombic cell. There are six planes corresponding to these lines. Dotted lines alternate between rectangles and circles, indicating directions that polarizations can take for monoclinic cells based on the simple cubic cell. There are three planes corresponding to these lines. Any polarization whose direction does not correspond to one of the three symbol types or four types of lines results from a triclinic-shaped cell.

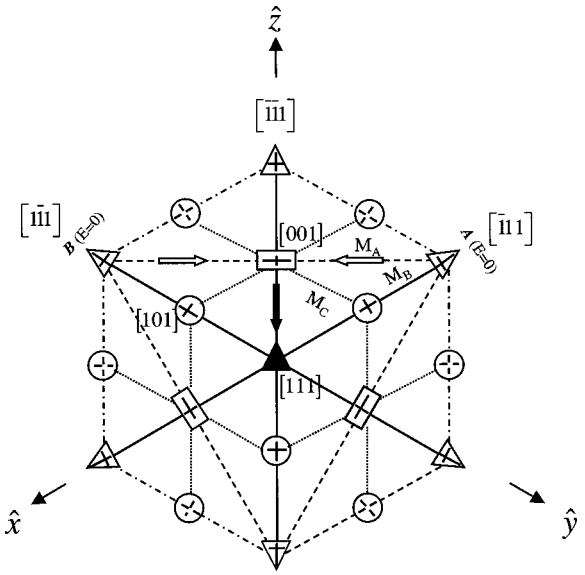

FIG. 2. Relations of various phases and the optical extinction orientations corresponding to polarizations along [111].

Most higher-symmetry phases (O, R, or T) with nearby polarization **P** directions are related directly by monoclinic phases. We now discuss examples pertinent to our later explanation of experimental results. Polarization **P** can be rotated continuously from the $[1\bar{1}\bar{1}]$ direction corresponding to an R domain, to the [111] direction corresponding to an R domain with **P** along E field, by means of a monoclinic M_B cell with highest-symmetry principal axis b_m along $[10\bar{1}]$. At the middle of this **P** rotation path is the O domain with **P** along [101], as can be seen in Fig. 2.

A less direct path for this **P** rotation, but apparently the one chosen by the crystal, consists of two steps. The first step consists of rotation of **P** from the R-domain $[1\bar{1}\bar{1}]$ direction to the T-domain [001] direction, by means of a monoclinic M_A cell with highest-symmetry principal axis b_m along [110]. The second step consists of rotation of **P** from the T-domain [001] direction to the R-domain [111] direction by means of continuous strain and **P** variation of another monoclinic M_A cell with highest-symmetry principal axis b_m

along $[1\bar{1}0]$. Note that there is no discontinuous change in M_A cell shape as **P** passes through the [001] direction. The b_m axis and the other long cell axis merely switch roles.

Figure 2 also presents a projection, along the optical propagation direction [111], of domain polarization directions. Domains that are optically neutral for **k** along [111] will have extinction for optical electric field along the radial and circumferential axes indicated by solid crossed lines inside the symbols. Dashed crossed lines inside some circles indicate that extinction will be incomplete because of optical activity for such *O* domains. Solid lines between some symbols indicate no shift in extinction directions away from those in symbols connected by these lines. Lines for the remaining $Z=2$ (dashed and dash-dot) and all $Z=1$ (dotted) *M* polarization directions indicate shift in optical extinction direction away from radial and circumferential. The central black triangle indicates total optical extinction for any optical field direction.

As shown in Fig. 1(a), at $E=0$ kV/cm, the domain matrix exhibits three different orientations of extinction as marked by *A*, *B* and *C*. Hereafter, the extinction angle of the "*A*" region at $E=0$ kV/cm is chosen as zero degrees (0°). "*B*" regions show optical extinction at 30°. "*C*" regions exhibit extinction at all P/A angles, indicating the *R* phase with the polarization along [111]. However, the "*D*" region does not show extinction at all, perhaps due to strong local strain distorting the index ellipsoid. When observing the (111)-cut sample along [111], between a crossed P/A pair, the rotation angle of extinction between adjacent *R* domains around the periphery of Fig. 2 (for instance: $[\bar{1}11]\leftrightarrow[\bar{1}\bar{1}1]$ or $[\bar{1}\bar{1}1]\leftrightarrow[1\bar{1}1]$) is 30°. One evidence that indicates domains of "*A*" and "*B*" regions to be rhombohedral is an observation under application of $E=12$ kV/cm [see Fig. 1(f)]. The domain matrix at $E=12$ kV/cm exhibits mostly extinction for all P/A angles, indicating a [111] rhombohedral phase as marked by R_{111}. The [111] *R* domain should be induced easily by an external E field on a (111)-cut crystal if the original phase is rhombohedral. Thus, domains in *A* and *B* regions are certainly rhombohedral at $E=0$ kV/cm.

The extinction angles exhibit apparent change in the region of 3.5–5 kV/cm. Near $E=3.5$ kV/cm, domains in *A* and *B* regions exhibit various extinction angles, such as 20°, 25° and 60°, indicating a mixed phase of *R* and *M* domains. Especially at $E=4.1$ kV/cm the 90° domain walls (associated with stripe-like lines) having extinction at 60°, appear for a short period of time (within minutes) in most domains, indicating *T* phases. While the E field stays at 4.1 kV/cm for a few minutes, as shown in Fig. 1(d), the 90° domain walls eventually disappear, and regions having extinction angle of 60° rapidly expand in the domain matrix. Near 5 kV/cm, most domains have the same extinction angle of 60°. This is consistent with the coercive field $E_C\sim 6$ kV/cm as shown in Fig. 1(i). Above 5 kV/cm, the crystal stays at the same extinction angle of 60° up to $E=12$ kV/cm, but the optical transmission is gradually reduced. The domain matrix shows total extinction at $E=12$ kV/cm, indicating that the crystal has reached the [111] R_{111} phase. Upon decreasing E field, as shown in Figs. 1(g) and 1(h), domains exhibit very different patterns compared with domains while increasing E field, showing an irreversible process. Extinctions at 15° or 10° occur for some domains, indicating that polarization rotations prefer monoclinic distortions as E field decreases.

What is the rotation path of domain polarizations as E field increases? As E field approaches 5 kV/cm, domain polarizations rotate through *M* phases toward the same extinction orientation of 60°. This indicates that extinction angles of *A* and *B* regions (at $E=0$) have, respectively, rotated 60° and 30°. One can visualize these movements of polarizations by rotating the crossed P/A pair. For instance, first align the polarizer of the P/A pair with the ***R*-*O*-*R*** solid line as indicated by "$A(E=0)$" in Fig. 2. In other words, the extinction angle for the *A* region is chosen as zero degrees (0°) as shown in Fig. 1(a). The bold "***R***" stands for the "black" triangle in Fig. 2. By rotating the P/A pair 30° counterclockwise, the analyzer of the P/A pair coincides with the extinction orientation of the domains whose polarizations point (from ***R***) to the ***R*-*O*-*R*** solid line as marked by "$B(E=0)$" in Fig. 2. Therefore, *A* and *B* regions show 30° difference in the extinction angles. As E field approaches 5 kV/cm, one reaches the extinction angle 60° with the polarizer of the P/A pair aligned with the ***R*-*T*-*R*** solid line between $A(E=0)$ and $B(E=0)$ by additional counterclockwise rotation of 30°, which corresponds to domain polarization rotation.

We see no apparent evidence for *O* domains as E field approaches 12 kV/cm, because they would give the same 0° and 30° extinction angles as *R* and *T* domains if the polarization rotation chose the path $R\rightarrow M_B\rightarrow O\rightarrow M_B\rightarrow R_{111}$ (solid lines in Fig. 2). However, *T* domains were evidenced at 4.1 kV/cm. Thus, in the region of 0–5 kV/cm, *R* domains most likely undergo M_A-type distortions and transform into *T* domains, i.e., $R\rightarrow M_A\rightarrow T$ as indicated by the "open" arrows in Fig. 2. Above $E=5$ kV/cm domains have almost the same extinction angle of 60° and turn gradually into total extinction as E field approaches 12 kV/cm. This indicates that domains transform into [111] R_{111} domains through another M_A distortion, i.e., $T\rightarrow M_A\rightarrow R_{111}$ as indicated by the black arrow in Fig. 2.

This work was supported by NSC Grant No. 91-2112-M-030-006 and DoD EPSCoR Grant No. N00014-02-1-0657.

[1] M. K. Durbin, E. W. Jacobs, J. C. Hicks, and S.-E. Park, Appl. Phys. Lett. **74**, 2848 (1999).
[2] D. Viehland, J. Appl. Phys. **88**, 4794 (2000).
[3] B. Noheda, Z. Zhong, D. E. Cox, G. Shirane, S.-E. Park, and P. Rehrig, Phys. Rev. B **65**, 224101 (2002).
[4] D. La-Orauttapong, B. Noheda, Z.-G. Ye, P. M. Gehring, J. Toulouse, D. E. Cox, and G. Shirane, Phys. Rev. B **65**, 144101 (2002).
[5] Y. Lu, D.-Y. Jeong, Z.-Y. Cheng, Q. M. Zhang, H. Luo, Z. Yin, and D. Viehland, Appl. Phys. Lett. **78**, 3109 (2001).
[6] D. Viehland and J. F. Li, J. Appl. Phys. **92**, 7690 (2002).
[7] Z.-G. Ye, B. Noheda, M. Dong, D. Cox, and G. Shirane, Phys. Rev. B **64**, 184114 (2001).
[8] J.-M. Kiat, Y. Uesu, B. Dkhil, M. Matsuda, C. Malibert, and G. Calvarin, Phys. Rev. B **65**, 064106 (2002).
[9] B. Noheda, D. E. Cox, G. Shirane, J. Gao, and Z.-G. Ye, Phys. Rev. B **66**, 054104 (2002).
[10] A. K. Singh and D. Pandey, Phys. Rev. B **67**, 064102 (2003).
[11] H. Fu and R. E. Cohen, Nature (London) **403**, 281 (2000).
[12] C.-S. Tu, V. H. Schmidt, I.-C. Shih, and R. Chien, Phys. Rev. B **67**, 020102(R) (2003).
[13] A. Sommerfeld, *Optics* (Academic, New York, 1964), pp. 129–139.
[14] N. H. Hartshorne and A. Stuart, *Crystals and the Polarizing Microscope* (Arnold, London, 1970).